Mini review

Electrochemical biosensors for the detection of matrix metalloproteinases

Jianlin Zhou [1,2]

[1] Hunan Province Key Laboratory of Coal Resources Clean-utilization and Mine Environment Protection, Hunan University of Science and Technology, Xiangtan, Hunan 411201, China
[2] School of Resource & Environment and Safety Engineering, Hunan University of Science and Technology, Xiangtan, Hunan 411201, China
E-mail: jianlinzhou_hnust@163.com

Matrix metalloproteinases (MMPs) involved in many physiological functions of human body have become the biomarkers and targets for early diagnosis and treatment prediction of many diseases. The methods for MMPs detection mainly include affinity assays and proteolytic reaction-based analysis. Electrochemical biosensors have attracted widespread interest due to their advantages of high sensitivity, simplicity, rapid response, and compatibility with miniaturization. In this view, the progress in the electrochemical strategies for MMPs detection was addressed, including affinity immunoassays and proteolytic reaction-based analysis.

1. INTRODUCTION

Extracellular matrix (ECM) is an extracellular component of tissue, which can provide support for cells, store growth factors, and regulate cell movement, intercellular interaction and intercellular communication [1]. It is composed of a variety of matrix macromolecules and the specific composition and structure of them vary from tissue to tissue. The main components of ECM include collagen, elastin, fibronectin, laminin, glycoprotein, proteoglycan and glycosaminoglycan. The formation and degradation of ECM play an important role in biological processes involving the maintenance of tissue homeostasis and regeneration. The enzymes to control the key physiological process are called matrix metalloproteinases (MMPs), zinc-dependent endonucleases to jointly cleave all components of ECM [2]. At present, a total of 24 MMPs have been identified in vertebrates, and most of them have been found to be expressed in humans [3]. Based on the substrate specificity in vitro, MMPs can be divided into seven categories: (1) collagenases (MMP-1, MMP-8, MMP-13 and MMP-18) which can cleave type I,

Int. J. Electrochem. Sci., 17 **(2022)** Article Number: 221034

2

II and III interstitial collagen, (2) gelatinases (MMP-2 and MMP-9) which can cleave the denatured collagen (gelatin) and the base membrane proteins, (3) stromalysins (MMP-3, MMP-10 and MMP-11) which can cleave laminin and other base membrane proteins, (4) matrilysins (MMP-7 and MMP-26) lacking carboxyl terminal domain which can cleave proteoglycans, laminin, elastin and type IV collagen, (5) membrane type MMPs expressed on the cell surface and connected to the plasma membrane through glycophosphatidylinositol anchors (MMP and MMP-25) or transmembrane domains (MMP-14, MMP-15, MMP-16 and MMP-24), (6) metalloelastase (MMP-12) which can cleave elastin and some base membrane proteins, and (7) other MMPs such as MMP-19, MMP-20, MMP-23 and MMP-28. The activity of MMPs is strictly regulated at transcriptional and post-translational levels as well as cell localization. When the balance interaction between MMPs and their inhibitors is affected, diseases such as inflammation, arthritis, periodontal disease, vascular disease, diabetes, fibrosis, tumor, hematological malignancy and neurosis may happen. Thus, MMPs have become the biomarkers and targets for early diagnosis and treatment prediction of many diseases [4].

MMPs are involved in many physiological functions of human body, such as cell proliferation, differentiation, apoptosis, immune function, tissue healing and angiogenesis [5]. The activity of MMPs is closely regulated in transcription, translation, enzymatic activation and the inhibition of regulatory proteins. The methods for MMPs detection mainly include affinity assays and proteolytic reaction-based analysis. For affinity determination, the detection and quantification of MMPs depends on the structure of proteases, which has no relationship with their activity. In contrast, proteolytic-reaction-based analysis is more meaningful for determining the function of MMPs. Moreover, in terms of the detection mode, protease analysis can be divided into homogeneous and heterogeneous analysis [6]. In homogeneous analysis, both the substrate and the sample exist in the aqueous phase. On the contrary, heterogeneous analysis requires the immobilization of the substrate on the solid surface. In heterogeneous analysis, a large number of substrate molecules can be fixed on the solid surface, thereby reducing the amount of samples and improving the sensitivity. In the sensing technique and concept, biosensors for the detection of MMPs include electrochemisty, surface plasmon resonance and other optical biosensors [7, 8]. Among them, electrochemical biosensors have attracted widespread interest due to their advantages of high sensitivity, simplicity, rapid response, and compatibility with miniaturization. Herein, the progress in the electrochemical strategies for MMPs detection was addressed, mainly including affinity immunoassays and proteolytic reaction-based analysis.

2. IMMUNOASSAYS

For the direct electrochemical immunoassays, the target-specific antibodies are attached on the electrode surface. The binding of targets to the antibodies can decrease the electron transfer rate, thus inducing the change in the potential, impedance or current [9]. Nanomaterials can increase the surface area of electrode and accelerate the electron-transfer rate to improving the sensitivity of electrochemical immunosensors (Table 1) [10]. For example, Liu et al. fabricated an immunosensor for MMP-1 detection using a gold nanoparticle/polyethyleneimine/reduced graphene oxide (AuNP/PEI/rGO)-modified disposable screen-printed electrode (SPE) [11]. The interaction between MMP-1 and its antibody limited the electron transfer of $[Fe(CN)_6]^{3-/4-}$, which could be monitored by differential pulse voltammetry

(DPV). The DPV response had a linear relationship with MMP-1 concentration in the range of 1 ~ 50 ng/mL with a detection limit of 0.219 ng/mL. Shabani et al. reported an impedance biosensor for MMP-9 detection using ZnO nanorod electrode [12]. The binding of MMP-9 with the antibody caused the change in charge transfer resistance, which was monitored by cyclic voltammetry (CV) and electrochemical impedance spectroscopy (EIS). The immunosensor exhibited a linear range of 1 ~ 1000 ng/mL. Yaiwong et al. reported an electrochemical immunosensor for the detection of MMP-7 using methylene blue (MB)-adsorbed molybdenum disulfide (MoS_2)/graphene oxide (GO) nanocomposite-deposited screen-printed carbon electrode (SPCE) [13]. The two-dimensional MoS_2/GO nanocomposite improved the electrode surface area, enhanced the exceptional electrical conductivity and accelerated the electron transfer. The binding of MMP-7 to the capture antibodies on the electrode surface led to the decrease in the peak current of MB. The immunosensor showed a linear logarithmic range from 0.01 to 75 ng/mL with a detection limit of 0.007 ng/mL. In addition, Nisiewicz et al. developed a three-dimensional (3D) platform for the detection of MMP-9 using G2 poly(amidoamine) dendrimer (PAMAM)-modified electrode [14].

Table 1. Analytical performances of different immunosensors for MMPs detection.

Electrode or signal reporter	Target	Detection limit	Linear range	Ref.
AuNP/PEI/rGO	MMP-1	0.219 ng/mL	1 ~ 50 ng/mL	[11]
ZnO nanorod	MMP-9	0.15 ng/mL	$1 \sim 1 \times 10^3$ ng/mL	[12]
MB/MoS_2/GO	MMP-7	0.007 ng/mL	0.01 ~ 75 ng/mL	[13]
PAMAM	MMP-9	2 pg·mL	$0.1 \sim 5 \times 10^3$ ng/mL	[14]
HRP/GO	MMP-2	0.01 pg/mL	$0.5 \sim 5 \times 10^4$ pg/mL	[15]
Poly-HRP	MMP-9	13 pg/mL	0.03 ~ 2 ng/mL	[16]
Poly-HRP	MMP-9	2.4 pg/mL	$8 \sim 1 \times 10^4$ pg/mL	[17]
Polymer/HRP	MMP-3	4 pg/mL	$4 \sim 3 \times 10^2$ pg/mL	[18]

In contrast to the direct detection format, sandwich immunoassay exhibits higher sensitivity and selectivity because of the use of two matched antibodies. To further improving the sensitivity, nanomaterials, enzymes and DNA nanostructures are usually employed to amplify the electrochemical signals [19-21]. Several enzyme-labeled sandwich immunosensors have been developed for the detection of different MMPs [15-18, 22, 23]. For example, Yang et al. designed a sandwich electrochemical immunosensor for MMP-2 detection using horseradish peroxidase (HRP)-loaded polydopamine-functionalized graphene oxide (GO) as the signal reporter [15]. The gold nanoparticle (AuNP)-attached nitrogen-doped graphene (NG) composite was used as the scaffold for the immobilization of MMP-2 antibodies. The immunosensor achieved the detection of MMP-2 in the concentration range of 0.5 pg/mL ~ 50 ng/mL with a detection limit of 0.11 pg/mL. Ruiz-Vega et al. developed an electrochemical magneto-immunosensor for MMP-9 detection with poly-HRP as the signal amplifier. The immunosensor determined MMP-9 at the concentration range of 0.03 ~ 2 ng/mL with a detection limit down to 13 pg/mL. They also used a paper device to develop a magneto-immunosensor for MMP-9 detection [16]. It was performed with a customized multiplexed holder

combined with eight screen-printed carbon electrodes (SPCEs) and a movable multiplexed fluidic module. The immunosensor exhibited a linear response of 0.03 ~ 2 ng/mL for MMP-9 quantification. Arévalo et al. reported the sandwich magneto-immunoassay of MMP-9 using screen-printed carbon electrode (SPCE) [17]. A commercial streptavidin-conjugated HRP polymers were used as the signal reporters. The immunoplatform achieved a detection limit of 2.4 pg/mL. Munge et al. proposed an electrochemical immunosensor for MMP-3 detection using vertically aligned single-wall carbon nanotube (SWCNT) electrode arrays [18]. Polymer beads loaded with multi-HRP and secondary antibody were used as the signal labels. The immunosensor showed a detection limit down to 4 pg/mL.

3. PROTEOLYTIC REACTION-BASED ANALYSIS

3.1 Impedance-based analysis

Electrochemical impedance spectroscope (EIS) is an inherently nondestructive and potentially sensitive technique to monitor the interfacial change, which has been widely utilized to detect small biomolecules, proteins, DNA and proteases in view of the advantages of label-free format, simple operation, and fast response. For this consideration, Palomar et al. developed a simple electrochemical MMP-7 biosensor by using peptide-decorated gold nanoparticle/carbon nanotube-modified gold electrode [24]. The negatively charged peptide on the electrode surface prevented the electron transfer of $[Fe(CN)_6]^{3-/4-}$. Cleavage of the peptide by MMP-7 reduced the impediment, thus allowing for the detection of MMP-7 with a detection limit of 6 pg/mL and a linear range of 10 pg/mL ~ 1000 ng/mL. Wang et al. developed an amperometric biosensor with polyaniline gel as the electrode modifier and Pb^{2+}-loaded carbon sphere (CS)-gold nanoparticle nanocomposite (CS-AuNP-Pb^{2+}) as the impedance enhancer [25]. The electrode showed excellent conductivity and large specific surface area for the redox of $[Fe(CN)_6]^{3-/4-}$. CS-AuNP-Pb^{2+} significantly increased the interfacial resistance and led to the enhancement of current difference (ΔI). Additionally, Pb^{2+} could react with tartrate monomers to generate non-conductive tartrate gels on electrode surface, resulting in the further enhancement of ΔI. Cleavage of peptide substrate by MMP-2 limited the production of tartrate gels and the amplification of ΔI. The biosensor showed a linear range of 1 pg/mL ~ 1 μg/mL. Recently, Zhang et al. reported a low-fouling platform for MMP-7 detection with urease@zeolite imidazole framework (urease@ZIF)-labeled peptide as the probe [26]. The SA-GO-Pb^{2+} gel was used to prepare the low-fouling electrode interface. The pyrrole doped urease@ZIF (urease@ZIF-Py) could catalyze the production of CO_2 by urea decomposition, thus producing $PbCO_3$ precipitation and leading to the decrease in the conductivity of electrode. The method showed good antifouling performance and achieved the detection of MMP-7 in the range of 0.1 pg/mL ~ 100 ng/mL with a detection limit of 24.34 fg/mL. In addition, Biela et al. proposed a disposable sensor for MMP-9 determination by coating the electrode with oxidized dextran [27]. The MMP-9-specific peptide was cross-linked on the electrode surface. Incubation of the film with MMP-9 caused the degradation of the cross-linked peptide film and the follow-up impedance change. MMP-9 was readily determined in a range of 50 ~ 400 ng/mL with a detection limit of 15 ng/mL.

3.2 Redox labels and nanocatalysts

Ferrocene (Fc), methylene blue (MB) and their derivatives exhibit well-defined electrochemical signals [28, 29], which can be readily labeled at the N- or C-terminal of peptide. Fc and MB-labeled peptides have been widely used to design biosensors for the detection of MMPs with high simplicity (Table 2). Xu et al. designed a ferrocenylacetic acid-labeled peptide substrate for the detection of MMP-2 with a detection limit of 0.3 ng/mL [30]. The peptide was anchored on the gold electrode surface and the signal was measured by differential pulse voltammetry (DPV). MMP-2 cleaved the peptide into two segments, thus resulting in the remove of Fc group and the decrease of the DPV signal. Sun et al. reported the determination of MMP-14 using an Fc-labeled peptide (CK11-Fc) as the probe [31]. Cleavage of CK11-Fc assembled on the electrode surface made Fc released from the electrode, thus causing the decrease in the electrochemical signal. The current decreased linearly with MMP-14 concentration in the range 0.2 ~ 0.9 ng/L, and the detection limit was found to be 0.1 ng/L. Recently, Nisiewicz et al. designed a voltammetric technique for MMP-9 determination by using ferrocene-labeled dipeptide glycine-methionine (Gly-Met-Fc) as the substrate [32]. The specific enzymatic cleavage of dipeptide led to the release of Fc moiety. The biosensor showed a wide linear range (2 pg/mL ~ 5 μg/mL) and a detection limit down to 0.04 pg/mL. Lee et al. reported the detection of MMP-9 with MB-labeled peptide as the substrate [33]. The peptide was immobilized onto the gold electrode through the Au-S interaction. Cleavage of the peptide by MMP-9 led to the release of electroactive MB from the electrode surface, thus causing the decrease in the peak current. The biosensor showed a linear curve in the concentration range of 1 pM ~ 1 nM and a detection limit of 7 pM. Shin et al. reported a peptide-based electrochemical biosensor for the detection of MMP-9 (Figure 1) [34]. The MB-labeled peptide substrate was assembled on the 300 μm diameter Au electrode. Cleavage of the peptide by MMP-9 led to the remove of MB from the electrode and thus caused a decrease in square wave voltammetry (SWV) signal. The detection limit of this method was 60 pM with a linear range up to 50 nM. The strategy with a redox-labeled peptide as the probe was then commonly applicable for the assays of other proteases. Wang et al. presented a strategy for MMP-2 detection through the dual-signal synergistic effect to improve the sensitivity [35]. Reduced graphene oxide-Au-poly(methylene blue) (rGO-Au-PMB) was used to modify the glass carbon electrode for the immobilization of peptide substrate. Pt nanoparticle-aminoferrocene-bovine serum albumin (PtNP-amFc-BSA) was coupled with the peptide to produce an electrochemical signal. Cleavage of the peptide substrate led to the increase of the peak current from MB and the decrease of the peak current from Fc. In addition, anthraquinone (AQ)-labeled peptide has also been used for the detection of MMP-2 with high sensitivity and stability [36].
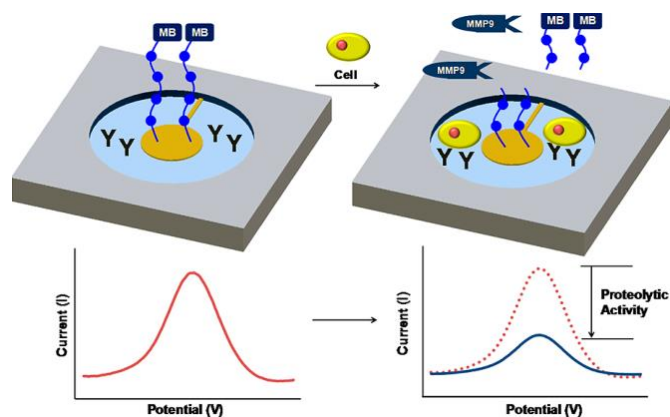
Figure 1. Scheme for the detection of MMP-9 release from monocytes. Copyright 2013 American Chemical Society [34].

Table 2. Analytical performances of proteolytic biosensors for MMPs detection.

Signal reporter	Target	Detection limit	Linear range	Ref.
Fc	MMP-2	0.3 ng/mL	$1 \sim 2 \times 10^2$ ng/mL	[30]
Fc	MMP-14	0.1 ng/L	$0.2 \sim 0.9$ ng/L	[31]
Fc	MMP-9	0.04 pg/mL	$2 \sim 5 \times 10^6$ pg/mL	[32]
MB	MMP-9	7 pM	$1 \sim 1 \times 10^3$ pM	[33]
MB	MMP-9	60 pM	$0.06 \sim 50$ nM	[34]
MB/Fc	MMP-2	Not reported	$0.01 \sim 10$ ng/L	[35]
AQ	MMP-2	10 fg/mL	$2 \sim 5 \times 10^6$ pg/mL	[36]
Fc polymer	MMP-2	0.53 fM	$8 \sim 8 \times 10^4$ fM	[37]
Fc polymer	MMP-2	0.27 pg/mL	$1 \sim 1 \times 10^3$ pg/mL	[38]
Fc-HRP/CB[7]@PtNPs	MMP-2	0.03 pg/mL	$0.1 \sim 2 \times 10^4$ pg/mL	[39]
CB[8]@AgNPs	MMP-2	0.12 pg/mL	$0.5 \sim 5 \times 10^4$ pg/mL	[40]
Au@Pt nanorods	MMP-2	0.18 ng/mL	$0.5 \sim 1 \times 10^2$ ng/mL	[41]
Thi/PtNPs	MMP-2	0.32 pg/mL	$0.001 \sim 10$ ng/mL	[42]
Pd-CNCs	MMP-7	17.38 fg/mL	$0.1 \sim 1 \times 10^5$ pg/mL	[43]
Thi/Pt/Pd/mhCeO$_2$	MMP-2	0.078 pg/mL	$1 \sim 1 \times 10^4$ pg/mL	[44]

To meet the requirement of signal-amplified detection, polymers formed by free radical polymerization have attracted great attention for the design of electrochemical biosensors. Wang et al. proposed an electrochemical biosensor for MMP-2 analysis with electrochemically mediated atom transfer radical polymerization (eATRP) for signal amplification [37]. The initiator of α-bromophenylacetic acid (BPAA) was labeled at the end of peptide substrate. The ATRP reaction was started with ferrocenylmethyl methacrylates (FMMA) with the help of copper activator to produce the ferrocene polymer. The cleavage of peptide by MMP-2 led to the release of the initiator, thus limiting the ATRP reaction on the electrode surface and leading to the decrease in the electrochemical signal of Fc. The peak current changed linearly with the MMP-2 concentration in the range of 8 fM ~ 80 pM. The detection limit was found to be 0.53 fM. Hu et al. proposed an electrochemical MMP-2 sensor by the electrochemically induced grafting of ferrocenyl polymer for signal readout [38]. The enzymatic

cleavage of peptide substrate on the electrode surface induced the generation of a free carboxyl group. Dithiobenzoate, 4-cyano-4-(phenylcarbonothioylthio)pentanoic acid (CPAD) as the reversible addition-fragmentation chain-transfer (RAFT) agent, was then attached on the electrode surface via the carboxylate-Zr(IV)-carboxylate interactions. This facilitated the grafting of ferrocenyl polymer through electrochemically induced RAFT (eRAFT) polymerization of ferrocenylmethyl methacrylate (FcMMA). The large number of redox Fc groups showed an amplified electrochemical signal, thus allowing for the quantification of MMP-2 with a detection limit of 0.27 pg/mL and a linear range of 1 pg/mL ~ 1 ng/mL.

The macrocyclic receptor of cucurbit[8] can tie up two aromatic amino-acid residues based on the host-guest interaction with high binding affinity. Silver nanoparticles (AgNPs) can be used as the signal reporters of electrochemical biosensors because of their low-redox potential and highly characteristic solid-state Ag/AgCl process [45]. Cheng et al. reported the determination of MMP-2 with a phenylalanine-contained peptide substrate, in which the phenylalanine-contained peptide-templated silver nanoparticles (AgNPs) were used as the signal reporters [40]. The peptide substrate was immobilized on the electrode surface to recruit the peptide-templated AgNPs through the host-guest interactions between phenylalanine and cucurbit[8]. The cleavage of peptide substrate by MMP-2 led to the release of peptide-templated AgNPs from the electrode surface, thus decreasing the peak current. The signal amplification by AgNPs allowed for the sensitive detection of MMP-2 in the range of 0.5 pg/mL ~ 50 ng/mL with a detection limit of 0.12 pg/mL. Based on the host-guest interaction, Kou et al. developed an electrochemical MMP-2 biosensor by using PtNPs to regulate interenzyme distance for efficient enzyme cascade amplification (Figure 2) [39]. In this work, the cucurbit[7]uril-functionalized PtNPs (CB[7]@PtNPs) were used to load Fc-labeled HRP and glucose oxidase (GOx) through the host-guest interaction between Fc and CB[7]. The PtNPs-mediated enzyme cascade reaction had high catalytic efficiency. The biosensor showed a linear range of 0.1 pg/mL ~ 20 ng/mL and a detection limit of 0.03 pg/mL. The strategy overcomes the shortcomings of unstable structure and complex preparation of traditional scaffolds including metal-organic framework (MOF) and DNA nanostructure.
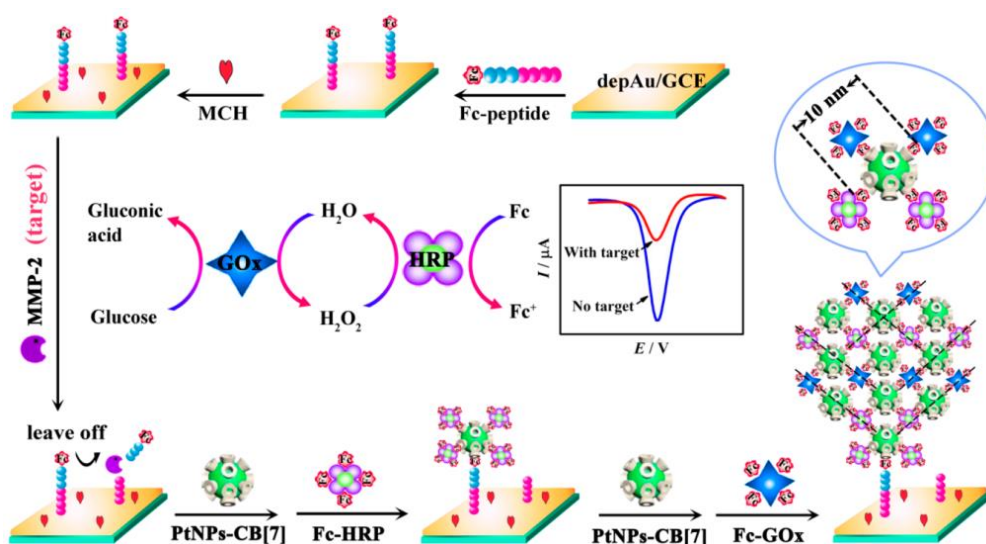
Figure 2. Schematic illustration of PtNPs regulated highly efficient enzyme cascade amplification for electrochemical detection of MMP-2. Copyright 2017 American Chemical Society [39].

Metallic nanomaterials can accelerate the electron transfer rate and exhibit catalytic activities .They can be used as the nanolabels to enhance the electrochemical signals, avoiding the shortcomings of enzyme labels (e.g. thermal and environmental instability) [46, 47]. Xi et al. proposed an H_2O_2-free electrochemical biosensor for MMP-2 detection using bimetallic Au@Pt nanoenzyme as the signal marker [41]. The bimetallic Au@Pt nanorods labeled at the peptide terminal could electrochemically catalyze the oxidation of TMB by O_2 in neutral pH. The biosensor showed a detection range of 0.5 ~ 100 ng/mL with a detection limit of 0.18 ng/mL. Jing et al. prepared a "signal on-off" electrochemical biosensor for MMP-2 determination [42]. DNA-modified PtNPs were immobilized on the electrode surface through the streptavidin-biotin interaction with peptide as the linker. Through hybridization chain reaction (HCR), a large number of electroactive thionine (Thi) molecules were embedded into the electrode surface. PtNPs effectively catalyzed the decomposition of H_2O_2, causing a significant increase in the electrochemical signal of Thi ("signal-on" state). When the peptide was cut by MMP-2, the PtNPs and electroactive Thi molecules were released from the electrode surface, leading to a significant decrease in the electrochemical signal ("signal-off" state). The sensor showed high sensitivity with a detection limit of 0.32 pg/mL. Wei et al. designed an amperometric biosensor for MMP-7 detection using Pd-functionalized carbon nanocomposites (Pd-CNCs) as the impedance enhancers [43]. The Pd-CNCs labeled at the peptide could catalyze the oxidation of 4-chloro-1-naphthol by H_2O_2 to produce insoluble precipitation on electrode surface. Moreover, the poorly conductive CNCs also increased the resistance and caused the significant decrease in the square wave voltammetry (SWV) current from $[Fe(CN)_6]^{3-/4-}$. Treating the electrode with MMP-7 caused the cleavage of peptide and thus promoted the increase of SWV current. Based on the signal difference before and after treatment of MMP-7, the SWV signal changed with MMP-7 concentration in the range of 100 fg/mL ~ 100 ng/mL. Xu et al. reported the detection of MMP-2 with bimetallic Pt and Pd nanoparticles-encapsulated mesoporous-hollow ceria nanospheres (Pt/Pd/mhCeO$_2$) as the nanocarriers and electrocatalysts [44]. Streptavidin (SA) and electroactive thionine (Thi) were loaded onto the Pt/Pd/mhCeO$_2$ nanospheres. Cleavage of the biotin-labeled peptide substrate on the AuNPs-modified electrode by MMP-2 limited the attachment of SA/Thi/Pt/Pd/mhCeO$_2$ through the SA-biotin interaction. In this method, the electrochemical signal was produced based on the catalytic decomposition of H_2O_2 by Pt/Pd/mhCeO$_2$ nanospheres. The result indicated that MMP-2 at the concentration of 0.1 pg/mL ~ 10 ng/mL could be readily determined with a detection limit of 0.078 pg/mL.

3.3 Others

Homogeneous electrochemical biosensors carried out in solution do not need the immobilization of probe on the electrode surface. The target can trigger the diffusion or adsorption of signal molecules on the electrode surface, so as to realize the simple, rapid and sensitive detection [48-50]. For this view, Duan et al. proposed a homogeneous method for the detection of MMP-2 activity using orderly distributed mesoporous silica films (MSFs)-modified electrode [51]. The positively charged peptide substrates were absorbed onto the surface of MSFs by electrostatic interactions, thus preventing electroactive $[Ru(NH_3)_6]^{3+}$ to approach the electrode. Without MMP-2, the peptide substrates would be enzymatically cleaved, allowing for the approaching of $[Ru(NH_3)_6]^{3+}$ to the electrode surface and causing the increase of the peak current. MMP-2 at the concentration of 0.98 ng/mL was readily

determined. Wang et al. developed an electrochemical biosensor for MMP-2 detection by converting the peptide cleavage event into DNA detection [52]. Exo III-assisted cycling signal amplification was used to improve the sensitivity. The peptide substrates modified on the surface of magnetic polystyrene microsphere (PSC-peptide) were coupled with DNA1-modified gold nanoparticles (AuNPs-DNA1). When the peptide was hydrolyzed by MMP-2, the AuNPs-DNA1 would be released from the surface of magnetic microsphere. The released AuNPs-DNA1 could hybridize with the MB-labeled DNA2 (MB-DNA2) to form DNA duplexes. The MB-DNA2 in the duplexes could be enzymatically cleaved by Exo III, thus leading to the release of small electroactive MB moiety. At the same time, the AuNPs-DNA1 were regenerated with the digestion of DNA2 and then hybridized with other MB-DNA2. Thus, one AuNP-DNA1 triggered the generation of numerous free MB tags that could approach to the CB[7]-modified electrode via host-guest interactions, producing an strong electrochemical signal.

Peptide with a specific sequence can self-assemble into various nanostructures under mild conditions [53]. Cleavage of peptide by protease may inhibit or accelerate the self-assembly of peptide substrate or its proteolytic product [54]. Wang et al. reported the detection of MMP-2 based on the self-assembly of peptide on ionic nanochannel [55]. The peptide substrate with a sequence of CPLGVRKLVFFKK can be assembled into network on the ionic nanochannel to cover the porous anodic alumina (PAA), thus producing an ion current rectification (ICR) effect. The digestion of peptide by MMP-2 led to the increase of ICR effect, which could be readily monitored by an electrochemical device. The method allowed for the detection of MMP-2 with a linear detection range of 10 fg/mL ~ 10 ng/mL and a detection limit down to 6.6 fg/mL.
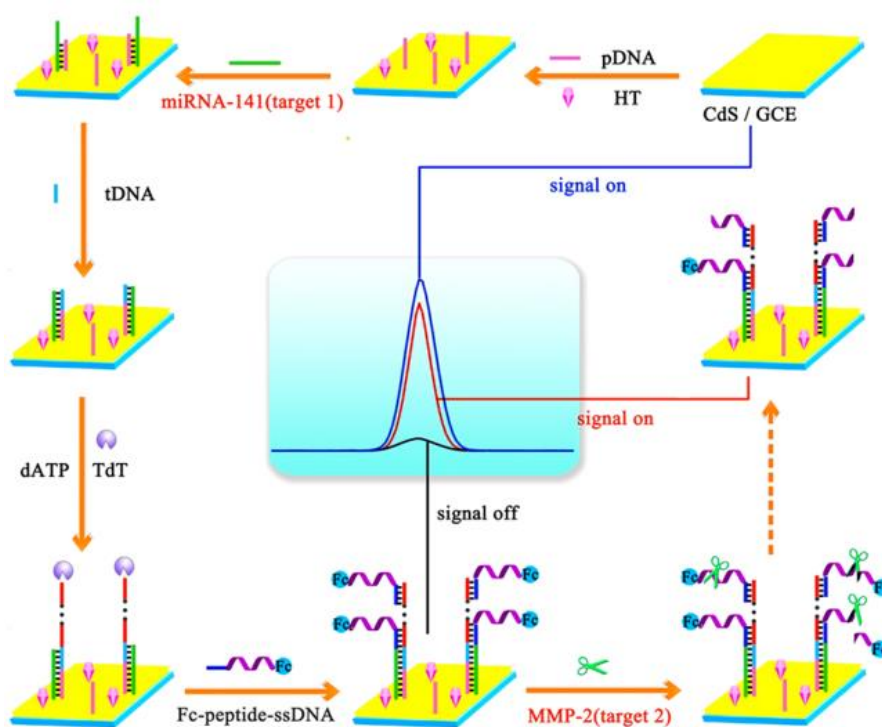
Figure 3. Fabrication of the ECL biosensing platform for the detection of multiple types of biomarkers on a single interface. Copyright 2017 American Chemical Society [56].

It is a challenge to detect multiple different types of biomarkers on a single interface. Through the "on-off-on" switch, target-induced cleavage and terminal deoxynucleoside transferase (TdT)-regulated extension, an ECL biosensor was proposed by Nie et al. for the detection of multiple biomarkers including MMP-2 and microRNA-141 (miRNA-141) (Figure 3) [56]. In this method, miRNA-141 was firstly hybridized with probe DNA (pDNA) attached on the surface of CdS QDs-modified interface. Then, the trigger DNA (tDNA) was captured by miRNA-141 to form a long ssDNA nanotail through the TdT-mediated DNA polymerization. The resulting ssDNA facilitated the binding of extensive Fc-peptide-ssDNA conjugates via hybridization. This led to the decrease of ECL intensity because of the high quenching effect of Fc to CdS QDs. In the presence of MMP-2, the Fc-peptide-ssDNA conjugate was digested and the Fc tag was then released from the sensor interface, thus enhancing the ECL signal. The method showed a detection limit of 33 fg/mL for MMP-2 analysis.

4. CONCLUSION

In summary, the methods for MMPs detection mainly include affinity immunoassays and proteolytic reaction-based analysis. According to the first method, the binding between MMPs and their antibodies can produce the signal change. The main advantage of immunoassays is the high selectivity for target. However, the antibodies-modified electrodes are expensive and need to be stored at low temperature to avoid denaturation. The second method based on the proteolysis of MMPs requires a sequence-specific peptide to generate the electrochemical signal. Once the peptide substrate is cut off, the signal will change substantially. In this way, the activity of MMPs can be measured, but the true selectivity of peptide sequence is questionable. So far, there is no commercial proteolytic reaction-based biosensors for MMPs in the market. This work should be valuable for the design of novel affinity and proteolytic biosensors for the detection of total and active MMPs.

References

1.   G. S. Hussey, J. L. Dziki and S. F. Badylak, *Nat. Rev. Mater.*, 3 (2018) 159.
2.   H. Nagase and J. F. Woessner, *J. Biol. Chem.*, 274 (1999) 21491.
3.   A. Jabłońska-Trypuć, M. Matejczyk and S. Rosochacki, *J. Enzym. Inhib. Med. Chem.* , 31 (2016) 177.
4.   R. Roy, J. Yang and M. A. Moses, *J. Clin. Oncol.* , 27 (2009) 5287.
5.   S. Löffek, O. Schilling and C.-W. Franzke, *Eur. Respir. J.*, 38 (2011) 191.
6.   I. L. H. Ong and K. L. Yang, *Analyst*, 142 (2017) 1867.
7.   Z. Lei, M. Jian, X. Li, J. Wei, X. Meng and Z. Wang, *J. Mater. Chem. B*, 8 (2020) 3261.
8.   A. Kirchhain, N. Poma, P. Salvo, L. Tedeschi, B. Melai, F. Vivaldi, A. Bonini, M. Franzini, L. Caponi, A. Tavanti and F. Di Francesco, *TrAC-Trend. Anal. Chem.*, 110 (2019) 35.
9.   Q. Zhang and L. Ou, *Int. J. Electrochem. Sci.*, 17 (2022) 220734.

10.   W. Wen, X. Yan, C. Zhu, D. Du and Y. Lin, *Anal. Chem.*, 89 (2017) 138.
11.   X. Liu, L. Y. Lin, F. Y. Tseng, Y. C. Tan, J. Li, L. Feng, L. Song, C. F. Lai, X. Li, J. H. He, R. Sakthivel and R. J. Chung, *Analyst*, 146 (2021) 4066.
12.   E. Shabani, M. J. Abdekhodaie, S. A. Mousavi and F. Taghipour, *Biochem. Eng. J.*, 164 (2020).
13.   P. Yaiwong, N. Semakul, S. Bamrungsap, J. Jakmunee and K. Ounnunkad, *Bioelectrochemistry*, 142 (2021) 107944.
14.   M. K. Nisiewicz, A. Kowalczyk, M. Sikorska, A. Kasprzak, M. Bamburowicz-Klimkowska, M. Koszytkowska-Stawińska and A. M. Nowicka, *Talanta*, 247 (2022) 123600.
15.   G. Yang, L. Li, R. K. Rana and J.-J. Zhu, *Carbon*, 61 (2013) 357.
16.   G. Ruiz-Vega, T. Garcia-Berrocoso, J. Montaner and E. Baldrich, *Sens. Actuat. B: Chem.*, 298 (2019) 126897.
17.   B. Arevalo, A. Ben Hassine, A. Valverde, V. Serafin, A. Montero-Calle, N. Raouafi, J. Camps, M. Arenas, R. Barderas, P. Yanez-Sedeno, S. Campuzano and J. M. Pingarron, *Talanta*, 225 (2021) 122054.
18.   B. S. Munge, J. Fisher, L. N. Millord, C. E. Krause, R. S. Dowd and J. F. Rusling, *Analyst*, 135 (2010) 1345.
19.   X. Pei, B. Zhang, J. Tang, B. Liu, W. Lai and D. Tang, *Anal. Chim. Acta*, 758 (2013) 1.
20.   C. Kokkinos, A. Economou and M. I. Prodromidis, *TrAC-Trend. Anal. Chem.*, 79 (2016) 88.
21.   Z. k. Farka, T. s. Juřík, D. Kovář, L. e. Trnková and P. Skládal, *Chem. Rev.*, 117 (2017) 9973.
22.   M. Ben Ismail, E. de la Serna, G. Ruiz-Vega, T. Garcia-Berrocoso, J. Montaner, M. Zourob, A. Othmane and E. Baldrich, *Anal. Chim. Acta*, 999 (2018) 144.
23.   E. de la Serna, E. Martínez-García, T. García-Berrocoso, A. Penalba, A. Gil-Moreno, E. Colas, J. Montaner and E. Baldrich, *Sens. Actuat. B: Chem.*, 269 (2018) 377.
24.   Q. Palomar, X. Xu, R. Selegård, D. Aili and Z. Zhang, *Sens. Actuat. B: Chem.*, 325 (2020) 325.
25.   H. Wang, Z. Ma and H. Han, *Bioelectrochemistry*, 130 (2019) 107324.
26.   Z. Zhang, Y. Xu, Y. Zhang, B. Ma, Z. Ma and H. Han, *Sens. Actuat. B: Chem.*, 364 (2022) 131844.
27.   A. Biela, M. Watkinson, U. C. Meier, D. Baker, G. Giovannoni, C. R. Becer and S. Krause, *Biosens. Bioelectron.*, 68 (2015) 660.
28.   N. Xia, D. Wu, T. Sun, Y. Wang, X. Ren, F. Zhao, L. Liu and X. Yi, *Sens. Actuat. B: Chem.*, 327 (2021) 128913.
29.   N. Xia, D. Wu, H. Yu, W. Sun, X. Yi and L. Liu, *Talanta*, 221 (2021) 121640.
30.   H. Xu, H. Ye, L. Yu, Y. Chi, X. Liu and G. Chen, *Anal. Methods*, 7 (2015) 5371.
31.   L. Sun, Y. Chen, F. Chen and F. Ma, *Microchem. J.*, 157 (2020) 105103.
32.   M. K. Nisiewicz, A. Kowalczyk, A. Gajda, A. Kasprzak, M. Bamburowicz-Klimkowska, I. P. Grudzinski and A. M. Nowicka, *Biosens. Bioelectron.*, 195 (2022) 113653.
33.   J. Lee, J. Y. Yun, W. C. Lee, S. Choi, J. Lim, H. Jeong, D.-S. Shin and Y. J. Park, *Sens. Actuat. B: Chem.*, 240 (2017) 735.
34.   D. S. Shin, Y. Liu, Y. Gao, T. Kwa, Z. Matharu and A. Revzin, *Anal. Chem.*, 85 (2013) 220.
35.   H. Wang and Z. Ma, *Sens. Actuat. B: Chem.*, 266 (2018) 46.
36.   M. K. Nisiewicz, A. Gajda, A. Kowalczyk, A. Cupriak, A. Kasprzak, M. Bamburowicz-Klimkowska, I. P. Grudzinski and A. M. Nowicka, *Anal. Chim. Acta*, 1191 (2022) 339290.
37.   Q. Wang, J. Liu, S. Yu, H. Sun, L. Wang, L. Li, J. Kong and X. Zhang, *Microchem. J.*, 164 (2021) 106015.
38.   Q. Hu, L. Su, Y. Mao, S. Gan, Y. Bao, D. Qin, W. Wang, Y. Zhang and L. Niu, *Biosens. Bioelectron.*, 178 (2021) 113010.
39.   B. B. Kou, Y. Q. Chai, Y. L. Yuan and R. Yuan, *Anal. Chem.*, 89 (2017) 9383.
40.   W. Cheng, J. Ma, D. Kong, Z. Zhang, A. Khan, C. Yi, K. Hu, Y. Yi and J. Li, *Sens. Actuat. B: Chem.*, 330 (2021) 330.
41.   X. Xi, M. Wen, S. Song, J. Zhu, W. Wen, X. Zhang and S. Wang, *Chem. Commun.*, 56 (2020) 6039.

42.   P. Jing, H. Yi, S. Xue, R. Yuan and W. Xu, *RSC Advances*, 5 (2015) 65725.
43.   Z. Wei, H. Wang, Z. Ma and H. Han, *Nanoscale Res. Lett.*, 13 (2018) 375.
44.   W. Xu, P. Jing, H. Yi, S. Xue and R. Yuan, *Sens. Actuat. B: Chem.*, 230 (2016) 345.
45.   C.-X. Yu, F. Xiong and L.-L. Liu, *Int. J. Electrochem. Sci.*, 15 (2020) 3869.
46.   L. Liu, D. Deng, W. Sun, X. Yang, S. Yang and S. He, *Int. J. Electrochem. Sci.*, 13 (2018) 10496.
47.   N. Xia, G. Liu, S. Zhang, Z. Shang, Y. Yang, Y. Li and L. Liu, *Analytica Chimica Acta*, 1214 (2022) 339965.
48.   N. Xia, T. Sun, L. Liu, L. Tian and Z. Sun, *Talanta*, 237 (2021) 122949.
49.   L. Liu, Y. Chang, X. Ji, J. Chen, M. Zhang and S. Yang, *Talanta*, 250 (2022) 123597.
50.   N. Xia, Z. Sun, F. Ding, Y. Wang, W. Sun and L. Liu, *ACS Sens.*, 6 (2021) 1166.
51.   S. Duan, J. Peng, H. Cheng, W. Li, R. Jia, J. Liu, X. He and K. Wang, *Talanta*, 231 (2021) 122418.
52.   D. Wang, Y. Yuan, Y. Zheng, Y. Chai and R. Yuan, *Chem. Commun.*, 52 (2016) 5943.
53.   N. Xia, Y. Huang, Y. Zhao, F. Wang, L. Liu and Z. Sun, *Sens. Actuat. B: Chem.*, 325 (2020) 128777.
54.   Y. Wang, L. Sha, H. Mao, J. Zhao and M. Tu, *Electrochim. Acta*, 411 (2022) 140100.
55.   L. Wang, H. Li, L. Shi, L. Li, F. Jia, T. Gao and G. Li, *Biosens. Bioelectron.*, 195 (2022) 113671.
56.   Y. Nie, P. Zhang, H. Wang, Y. Zhuo, Y. Chai and R. Yuan, *Anal. Chem.*, 89 (2017) 12821.